OPEN ACCESS
Modern Physics Letters A
Vol. 38, No. 6 (2023) 2350039 (9 pages)

DOI: 10.1142/S0217732323500396

Planck formula for the gluon parton distribution in the proton

Loredana Bellantuono*,†,¶, Roberto Bellotti†,‡ and Franco Buccella§

*Dipartimento di Biomedicina Traslazionale e Neuroscienze (DiBraiN), Università degli Studi di Bari Aldo Moro, Bari I-70124, Italy
†Istituto Nazionale di Fisica Nucleare, Sezione di Bari, Bari I-70125, Italy
‡Dipartimento Interateneo di Fisica, Università degli Studi di Bari Aldo Moro, Bari I-70126, Italy
§Istituto Nazionale di Fisica Nucleare, Sezione di Napoli, Napoli I-80126, Italy
¶loredana.bellantuono@ba.infn.it

Received 27 April 2022
Revised 31 March 2023
Accepted 25 April 2023
Published 7 June 2023

In this paper, we describe the gluon parton distribution function (PDF) in the proton, deduced by data from the ATLAS and HERA experiments, in the framework of the parton statistical model. The best fit parameters involved in the Planck formula that describes the gluon distribution are consistent with the results obtained from analysis of LHC deep inelastic proton–proton scattering processes. Remarkably, the agreement between the statistical model and the experimental gluon distributions is obtained with the same value of the "temperature" parameter $\bar{x}$ found by fitting the valence parton distributions from deep inelastic scattering. This result corroborates the validity of the statistical approach in the gluon sector.

Keywords: Gluons; partons; statistical parton model.

1. Introduction

The scale invariance in deep inelastic scattering of leptons (electrons, muons and neutrinos) on nucleons[1,2] had a crucial role in the proposal of quantum chromodynamics (QCD)[3] as the field theory of strong interactions. To describe the phenomenon, Feynman[4] proposed that the hadrons behave at large Q^2 as an incoherent set of point-like objects, called *partons*, characterized by a given probability of carrying a fraction $x \in [0, 1]$ of the hadron longitudinal momentum in the rest

¶Corresponding author.

frame of the final hadrons. While the charged partons have been identified with the quarks,[5] a relevant fraction of the hadron momentum is carried by neutral partons, identified with the gluons, that play the role of gauge bosons of QCD. The Q^2 dependance of the parton distributions is implied by QCD, as described by the DGLAP equations,[6–9] which have been experimentally confirmed.[10] Therefore, if one fixes an initial Q_0^2, sufficiently high that perturbative QCD is reliable, for larger values the parton distributions can be derived as a function of Q^2 by the DGLAP equations.

Polynomial functions are often considered for the boundary conditions, but theoretical ideas inspired by experimental facts suggest a different parametrization. The idea that Pauli principle implies $\bar{d}(x)$ larger than $\bar{u}(x)$[11,12] has been confirmed by the defect[13] in the Gottfried sum rule[14] and by the experiments on Drell–Yan production of lepton pairs in proton–proton and proton–deuteron scattering.[15,16] This fact has inspired to write parton distributions for the boundary low-Q^2 conditions[17] of DGLAP equations according to quantum statistical mechanics[18] in the variable x, which appears in the parton model sum rules. The "potentials" that appear in the Fermi–Dirac distributions of the valence partons depend on flavor ($q = u, d$) and helicity ($h = +, -$). This feature determines the intriguing possibility to describe both the unpolarized fermion distributions $q(x) = q^+(x) + q^-(x)$ and their polarized counterparts $\Delta q(x) = q^+(x) - q^-(x)$.[18–20]

An important constraint to the model is the hypothesis that, at the separation between the nonperturbative and the perturbative QCD regimes, there is equilibrium[21–23] for the elementary processes involved in the DGLAP equations. As a consequence, gluons must be described by a Planck formula, namely a Bose–Einstein distribution with vanishing chemical potential, while the isospin and spin asymmetries of the sea are related to the non-diffractive contribution to the valence parton distributions. This feature allows to predict, in agreement with the experiment (see Refs. 16 and 24)

$$\Delta\bar{d}(x) < 0 < \Delta\bar{u}(x) < \bar{d}(x) - \bar{u}(x) < \Delta\bar{u}(x) - \Delta\bar{d}(x). \tag{1}$$

Deep inelastic processes are unable to probe the gluon distribution with precision, since gluons, that are singlets with respect to the electroweak group, appear in the logarithmic correction of the parton distributions of the fermions, and their main constraint comes from the moment sum rule. Instead, they play an important role, as an octet of $\mathrm{SU}(3)_c$, in the strong $p-p$ interactions measured at the Large Hadron Collider (LHC), which is a "gluon factory". Purpose of this paper is to describe the parton distribution deduced by the measurements at ATLAS[25] and HERA[26] in the light of the statistical model. More specifically, we will determine the parameters of the statistical gluon distribution by fitting experimental data, and compare the result with the outcomes of previous studies, which were obtained from constraints on QCD sum rules and by their role in the DGLAP equations.

This paper is organized as follows. In Sec. 2, we introduce the statistical model and briefly discuss previous findings concerning both the fermion and gluon sectors.

Table 1. Values of the statistical model parameters found in previous works. The temperature $\bar{x}$ is involved in both the fermion and gluon distributions. The "potentials" X_u^+, X_u^-, X_d^+ and X_d^- determine the non-diffractive parts of the fermion distributions, while $\tilde{A}$ and $\tilde{b}$ fix the diffractive ones. Finally, A_G and b_G appear in the gluon distribution. We do not report the uncertainties, since they are not given in Refs. 18 and 28 and are underestimated in Ref. 27.

Parameter	Bourrely 2002[18]	Bourrely 2015[27]	Buccella 2015[28]
$\bar{x}$	0.099	0.090	0.102
X_u^+	0.461	0.475	0.446
X_u^-	0.298	0.307	0.297
X_d^+	0.228	0.245	0.222
X_d^-	0.302	0.309	0.320
A_G	14.28	32.8	27.18
b_G	0.747	1.02	1 (fixed)
$\tilde{A}$	0.083	0.147	0.07
$\tilde{b}$	−0.253	0.043	−0.25

In Sec. 3, we perform the fit of the gluon distribution function. In Sec. 4, we summarize the results and discuss their relevance.

2. Parton Statistical Model

The statistical model on which our analysis is based is built on a physically motivated picture, in which the nucleon is considered as a gas of massless partons, thermalized in a finite size volume.[18] Each parton is characterized by a statistical distribution function $p(x)$, whose parameters are determined at a given input energy scale Q^2. The general form of each distribution $p(x)$ reads

$$\left[\exp\left(\frac{x - X_p}{\bar{x}}\right) \pm 1\right]^{-1}, \tag{2}$$

with the plus sign holding for quarks and antiquarks (Fermi–Dirac distributions) and the minus sign for gluons (Bose–Einstein distribution). The constant X_p plays the role of a thermodynamical potential characterizing each parton p, while $\bar{x}$ is a universal *temperature* parameter, which is assumed to be the same for all the partons in a thermalized nucleon. Therefore, an important check of the model validity is to determine if the different parton distributions can be consistently fitted by the same temperature parameter.

The parameters of the statistical model found in the seminal work[18] at $Q^2 = 4\ \mathrm{GeV}^2/c^4$ were successfully used to describe the polarized nucleon structure functions.[19,20] Following studies[27] determined the same parameters at $Q^2 = 1\ \mathrm{GeV}^2/c^4$ and by comparison[28] with the parton distributions proposed in Ref. 26. We report in Table 1 the values, found in the aforementioned studies, of the relevant parameters

characterizing the quark and antiquark distributions[18]

$$xq^h(x) = \frac{AX_q^h x^b}{\exp[(x - X_q^h)/\bar{x}] + 1} + \frac{\tilde{A}x^{\tilde{b}}}{\exp(x/\bar{x}) + 1}, \tag{3}$$

$$x\bar{q}^h(x) = \frac{\bar{A}(X_q^{-h})^{-1}x^{2b}}{\exp[(x + X_q^{-h})/\bar{x}] + 1} + \frac{\tilde{A}x^{\tilde{b}}}{\exp(x/\bar{x}) + 1}, \tag{4}$$

(with $q = u, d$ and $h = +, -$) and the gluon distribution[18]

$$xg(x) = \frac{A_G x^{b_G}}{\exp(x/\bar{x}) - 1}. \tag{5}$$

The factors in the first terms of the fermion distributions may be explained by the extension to the transverse degrees of freedom[30,31] exactly for X_q^h and approximately for $(X_q^{-h})^{-1}$. The comparison among the parameters found in Refs. 18, 27 and 28 shows stability for $\bar{x}$, which we denote as the "temperature" of the model, and for the "potentials" X_q^h of the valence partons, depending on their flavor and helicity. Instead, the parameters A_G and b_G, which appear in the Planck distribution (5) of the gluons, are characterized by a more striking variability. The same occurs for the parameters $\tilde{A}$ and $\tilde{b}$ that determine the diffractive term of the fermion distributions. The discrepancy of Ref. 27 with respect to Ref. 18 is due to the choice of a smaller Q^2, lying in a region, where the gluon and diffractive distributions are expected to become narrower as a consequence of scale dependence. In the case of Ref. 28, differences are due to the fact that the parameters of the statistical model were fixed to match the distributions proposed in Ref. 26. In fact, the factor $(1-x)^C$ of the empirical parametrization and the Boltzmann factor $\exp(-x/\bar{x})$ has a different behavior, as stressed in Ref. 17, where the statistical description has been shown to be in a better agreement with the gluon distribution found in Ref. 29. The agreement found in Ref. 28 for the quark distributions of Ref. 26, but not for the gluon distributions above $x = 0.2$ leads us to compare the Planck form introduced in Ref. 18 with the distribution found by ATLAS,[25] where gluons, a $SU(3)_c$ octet, directly contribute to physical processes, which also include jets, while in the deep inelastic processes their role is limited to the logarithmic violations of scaling invariance implied by the DGLAP equations. It is thus crucial to determine the gluon distribution measured at ATLAS[25] at the same $Q^2 = 4\ \mathrm{GeV}^2/c^4$ considered in Ref. 18. In fact, while in deep inelastic scattering with incident leptons, gluons, that are singlets with respect to the electroweak gauge group, are fixed by their role in the DGLAP equations,[6–9] in proton–proton scattering they interact strongly as color octets. Therefore, one can hope to gain more information on the gluon distribution from LHC experiments. For this reason, we compare the prediction of the statistical approach with the experimental values, where they do not depend on the extrapolation following from the parametrization.

The slightly larger "potentials" and the large difference observed for the gluon and the diffractive terms may be the consequence of a different value of Q^2 chosen

in Ref. 27, since the distributions are modified by the evolution, which implies a narrowing of the distributions at increasing Q^2, and by the comparison with the very different parametrization of HERA for the gluons: in fact the comparison with NNPDF[29] shows a better agreement for Eq. (5).

3. Fit of the Gluon Distribution Function

Since we assume $Q_0^2 = 4\ \mathrm{GeV}^2/c^4$, we choose to limit the x range to $[0.05, 0.66]$, where the lower bound is fixed to avoid the QCD corrections proportional to $\alpha_s(Q_0^2)|\ln x|$, while the upper bound ensures that the invariant mass:

$$(M')^2 = M_p^2 + Q_0^2 \frac{1-x}{x}, \tag{6}$$

with M_p the proton mass, is not too small. At smaller and larger x, the proposed gluon distribution is more sensitive to parametrization. Moreover, at high x the experimental information is scarce; at small x, instead, the quark distributions given in Ref. 25 are characterized by $d(x) > u(x)$, a feature that cannot be obtained in the statistical approach, since the diffractive contribution must be equal in both distributions to avoid a divergence in the Gottfried sum rule, while the inequalities for the "potentials" imply that the non-diffractive contribution is larger for $u(x)$ than for $d(x)$.

Our choice to consider the range $(0.05, 0.66)$ is rather optimistic, since at $Q_0^2 = 4\ \mathrm{GeV}^2/c^4$, $\alpha(Q_0^2)|\ln 0.05| \simeq 0.9$ is not so small, and $(M')^2(x = 0.66) = (1.7)^2\ \mathrm{GeV}^2/c^4$ is a value in the region of the resonances, but the agreement shown in Fig. 1 and the precocious scaling justifies our assumption. With the increase of Q^2, the range of validity of the parton model increases on both sides, and we have the reasonable expectation that the extension of the parton distributions to the range $x \in (0, 1)$ has little influence on the evolution implied by the DGLAP equations.

We choose to fit the central values of the gluon momentum distribution $xg(x)$ obtained in the ATLAS experiment with free parameters A_G and b_G, and $\bar{x}$ fixed to the value determined in Ref. 18 by the rapidity of the decrease of the fermionic parton distributions around their "potentials" and above them. The best fit of $N = 74$ points in $[0.05, 0.66]$, obtained by least-square minimization, provides

$$A_G = 15.853 \pm 0.225, \quad b_G = 0.792 \pm 0.006. \tag{7}$$

The agreement of this result with the experimental points is reported in Fig. 1. The error bars therein are determined by three kinds of uncertainties, obtained from Ref. 25, that are summed in quadrature: the first kind is obtained from variations of the experimental parameters; the second is related to uncertainties in the physical constants, such as the quark mass and the coupling constants, of the physical model; the third one is determined by variations in the form of the fit function that provides the central value of the gluon distribution function in the ATLAS experiment.[25]

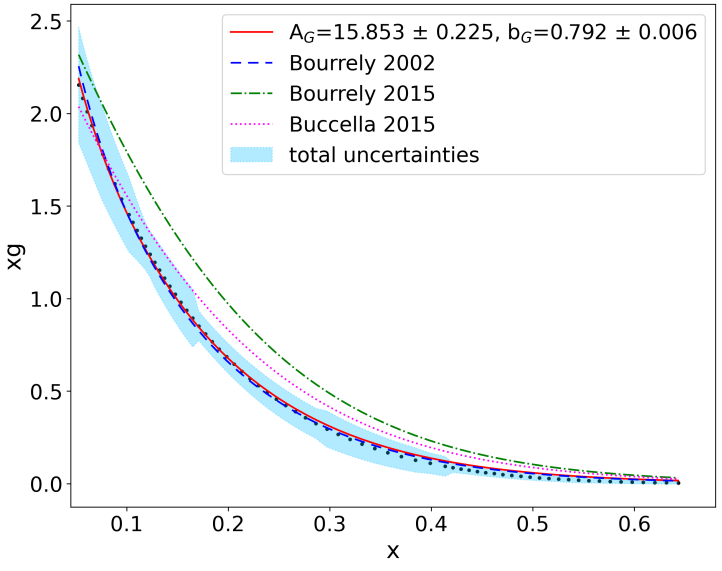

Fig. 1. (Color online) The solid red line represents the best fit of the gluon momentum distribution $xg(x)$ obtained in the ATLAS experiment, performed using the functional form in Eq. (5), with A_G and b_G as free parameters, and $\bar{x} = 0.099$. The dots correspond to the experimental points, and the (cyan) shaded area to their uncertainty. The curves obtained from the parameters in Ref. 18 (dashed blue line), Ref. 27 (dot-dashed green line), and Ref. 28 (dotted magenta line) in the same range are reported for comparison.

The visual agreement between the best fit and the reference points is confirmed by the value of $\chi^2 = 49.03$ (obtained by treating the uncertainties on the PDF as uncorrelated), which, considering the number $\nu = N - 2 = 72$, corresponds to a significance level close to 0.975. Adding $\bar{x}$ as a free parameter would lead to a lower χ^2, but also to a different temperature for quarks and gluons, inconsistent with the model.

The agreement with the values

$$A_G = 14.28, \quad b_G = 0.75, \tag{8}$$

found in Ref. 18 may be better understood, despite the fact that the uncertainties on the values of the parameters are not given in that paper, by comparing in Fig. 1 the curves corresponding to the central values in Eq. (7) (solid red line) and Eq. (8) (blue dashed line). One should also consider that in the aforementioned work the parameters of the gluon distribution were not fixed directly by a best fit operation, but rather on theoretical grounds, with b_G determined by the parameter $\tilde{b}$, appearing in the diffractive light-quark contribution, as $b_G = \tilde{b} + 1$, and A_G obtained from the momentum sum rule. The fact that similar parameters to the ones in Eq. (8) are obtained by fitting the ATLAS data for the gluon distribution is remarkable, and confirms the validity of the statistical approach.

Table 2. Integrated gluon momentum distributions for the model obtained in our work and for previous works. The results obtained in this work agree, within their errors, with all the ones reported in the second column.

	This work	Bourrely 2002[18]	HERA[26]	Buccella 2019[17]
$M_{g,\text{low}}$	0.358 ± 0.012	0.37	0.36	0.34
$M_{g,\text{high}}$	0.084 ± 0.002	0.08	0.05	0.13
M_g	0.442 ± 0.014	0.45	0.41	0.47

We report in Table 2 the values of the integrated momentum distribution for low ($x < 0.2$) and high ($x > 0.2$) momentum values

$$M_{g,\text{low}} = \int_0^{0.2} xg(x)dx, \quad M_{g,\text{low}} = \int_{0.2}^1 xg(x)dx, \tag{9}$$

along with the total momentum

$$M_g = \int_0^1 xg(x)dx = M_{g,\text{low}} + M_{g,\text{high}}, \tag{10}$$

carried by the gluons, using the best fit values (7). The comparison with the values obtained in Refs. 18, 26 and 17 confirms that the prediction of the gluon distribution fit is in a very good agreement, within the uncertainties of our model, with the one obtained in Ref. 18 and the shape significantly differs from the one proposed by Ref. 26. More specifically, there is good agreement at small x, but the difference becomes striking with increasing x. This effect is a consequence of the different behavior of the functions $\exp(-x/\bar{x})$ and $(1-x)^C$, that predict the large x gluon distributions in the statistical and in the standard empirical approach, respectively. The good agreement with data of the Planck formula is a good point in favor of the statistical approach, considering furthermore that it is obtained considering the value of $\bar{x}$ found from the form of the Fermi–Dirac function for the non-diffractive term of the valence partons.

4. Conclusions

The good agreement of the Planck formula for the gluon parton distribution in the proton with experiment with the value for the "temperature", $\bar{x} = 0.099$, and the other parameters, A_G and b_G near to the ones found in the study of deep inelastic scattering about 20 years ago, is a good point in favor of the parametrization inspired by quantum statistical mechanics, which allows a reliable extrapolation to the x regions, where one has not a sufficient information from experiment.

The agreement shown in Fig. 1 is still more remarkable considering that in Ref. 25 data are empirically fitted using the difference of two functions of the form $Ax^B(1-x)^C$, with the first one multiplied by a polynomial $P(x)$. The proposal of boundary conditions for the DGLAP equations[6–9] based on the principles of quantum statistical mechanics,[17] advocated in Refs. 11 and 12, receives an important

confirmation from the study of ATLAS data. For the low-x region, the diffractive term, which does not contribute to the parton model sum rules for the first moments, avoids the undesired contributions following from the statistical uncertainties (fluctuations in the difference of two infinite quantities are very dangerous!). For the intermediate- and high-x regions, the behavior of the Fermi–Dirac and Planck formulas, which is theoretically motivated, appears to describe the parton distributions better than the $(1-x)^C$ factors commonly used, and is expected to reduce the uncertainties in the high-x regions, where one has not enough experimental information. To check the stability of the free parameters in the Planck formula, we plan to extend our research by considering the gluon parton distributions proposed in Refs. 32–34.

Acknowledgments

We are very grateful to Francesco Giuli for informing us about the results reported in Ref. 25 and for providing the gluon distributions at $Q^2 = 4\ \mathrm{GeV}^2/c^4$. We thank Werner Vogelsang for the results reported in Ref. 24.

References

1. J. D. Bjorken and E. A. Paschos, *Phys. Rev.* **185**, 1975 (1969).
2. J. D. Bjorken and E. A. Paschos, *Phys. Rev. D* **1**, 3151 (1970).
3. H. Fritzsch, M. Gell-Mann and H. Leutwyler, *Phys. Lett. B* **47**, 365 (1973).
4. R. P. Feynman, *Photon-Hadron Interactions* (Taylor & Francis, 1972).
5. C. H. Llewellynn Smith, *Phys. Rep. C* **3**, 264 (1974).
6. V. N. Gribov and L. N. Lipatov, *Sov. J. Nucl. Phys.* **15**, 138 (1972).
7. L. N. Lipatov, *Sov. J. Nucl. Phys.* **20**, 94 (1975).
8. Y. Dokshitzer, *Sov. Phys. JETP* **46**, 641 (1977).
9. G. Altarelli and G. Parisi, *Nucl. Phys. B* **126**, 298 (1978).
10. G. Altarelli, *Phys. Rep.* **81**, 1 (1982).
11. A. Niegawa and K. Sasaki, *Progr. Theor. Phys.* **54**, 192 (1975).
12. R. D. Field and R. P. Feynman, *Phys. Rev. D* **15**, 2590 (1977).
13. NMC Collab. (M. Arneodo *et al.*), *Phys. Rev. D* **50**, R1 (1994).
14. K. Gottfried, *Phys. Rev. Lett.* **18**, 1174 (1967).
15. NA51 Collab. (A. Baldit *et al.*), *Phys. Lett. B* **332**, 244 (1994).
16. SeaQuest Collab. (J. Dove *et al.*), *Nature* **590**, 561 (2021).
17. F. Buccella, S. Sozha and F. Tramontano, *J. Stat. Mech.: Theory Exp.* **2019**, 073302 (2019).
18. C. Bourrely, J. Soffer and F. Buccella, *Eur. Phys. J. C* **23**, 487 (2002).
19. C. Bourrely, F. Buccella and J. Soffer, *Mod. Phys. Lett. A* **18**, 771 (2003).
20. C. Bourrely, F. Buccella and J. Soffer, *Eur. Phys. J. C* **41**, 327 (2005).
21. R. S. Bhalerao, *Phys. Lett. B* **380**, 1 (1996).
22. R. S. Bhalerao, N. G. Kelbar and B. Ram, *Phys. Lett. B* **476**, 285 (2000).
23. R. S. Bhalerao, *Phys. Rev. C* **63**, 025208 (2001).
24. STAR Collab. (L. Adamczyk *et al.*), *Phys. Rev. Lett.* **113**, 072301 (2014).
25. ATLAS Collab. (G. Aad *et al.*), *Eur. Phys. J. C* **82**, 438 (2022).
26. H1 and ZEUS Collab. (F. D. Aaron *et al.*), *JHEP* **2010**, 109 (2010).
27. C. Bourrely and J. Soffer, *Nucl. Phys. A* **941**, 307 (2015).

28. F. Buccella and S. Sohaily, *Mod. Phys. Lett. A* **30**, 1550203 (2015).
29. NNPDF Collab. (R. D. Ball *et al.*), *Eur. Phys. J. C* **77**, 663 (2017).
30. C. Bourrely, F. Buccella and J. Soffer, *Mod. Phys. Lett. A* **18**, 143 (2006).
31. C. Bourrely, F. Buccella and J. Soffer, *Int. J. Mod. Phys.* **28**, 13500 (2013).
32. T. J. Hou *et al.*, *Phys. Rev. D* **103**, 014013 (2021).
33. S. Bailey, T. Cridge, L. A. Harland-Lang, A. D. Martin and R. S. Thorne, *Eur. Phys. J. C* **81**, 341 (2021).
34. R. D. Ball *et al.*, *Eur. Phys. J. C* **82**, 428 (2022).